UAB-FT-429
KA-TP-6-99
hep-ph/9906268
June 1999

FCNC top quark decays in the MSSM: a door to SUSY physics in high luminosity colliders?

Jaume Guasch[*†]

Institut für Theoretische Physik
Universität Karlsruhe, D-76128 Karlsruhe, Germany

Joan Solà[‡]

Grup de Física Teòrica and Institut de Física d'Altes Energies, Universitat Autònoma de Barcelona, E-08193, Bellaterra (Barcelona) Catalonia, Spain

ABSTRACT

We study the FCNC top quark decays $t \to c\,h$ in the framework of the MSSM, where $h \equiv h^0, H^0, A^0$ is any of the supersymmetric neutral Higgs bosons. We include the leading set of SUSY-QCD and SUSY electroweak contributions. While the FCNC top quark decay into the SM Higgs boson has such a negligible rate that will not be accessible to any presently conceivable accelerator, we find that there is a chance that the potential rates in the MSSM can be measured at the high luminosity colliders round the corner, especially at the LHC and possibly at a future LC, but we deem it difficult at the upgraded Tevatron. In view of the large SUSY-QCD effects that we find in the Higgs channels, and due to some discrepancies in the literature, we have revisited the FCNC top quark decay into gluon, $t \to c\,g$, in our framework. We confirm that the possibility of sizeable rates does not necessarily require a general pattern of gluino-mediated FCNC interactions affecting both the LH and the RH sfermion sectors – the LH one being sufficient. However, given the present bounds on sparticle masses, the gluon channel turns out to lie just below the expected experimental sensibility, so our general conclusion is that the Higgs channels $t \to c\,h$ (especially the one for the light CP-even Higgs) have the largest potential top quark FCNC rates in the MSSM, namely of order 10^{-4}.

[*]Electronic address: guasch@itp.uni-karlsruhe.de
[†]On leave from Grup de Física Teòrica and Institut de Física d'Altes Energies, Universitat Autònoma de Barcelona, E-08193, Bellaterra (Barcelona) Catalonia, Spain.
[‡]Electronic address: sola@ifae.es

1 Introduction

The study of the virtual effects in top quark decays into Higgs bosons could be the clue to physics beyond the Standard Model (SM). This fact has already been demonstrated for top quark decays into charged Higgs bosons, $t \to H^+b$ [1], within the context of the Minimal Supersymmetric Standard Model (MSSM)[2][1]. Indeed, the potential existence of large quantum effects induced by supersymmetric particles in certain regions of parameter space may lead to highly significant changes in the partial width of that decay, and this feature could have a serious impact on the Higgs searches at the Tevatron [4, 5]. A situation which is in contrast to the SM decay of the top quark, $t \to W^+ b$, where the SUSY quantum effects are in general much more modest [6].

Similarly, one may expect that the top quark decays into the neutral Higgs bosons of the MSSM may undergo relevant enhancements. Notice, however, that in contradistinction to the charged current decays mentioned above, the loop contributions are in this case the lowest order effects as the neutral Higgs decays of the top quark are mediated by Flavor Changing Neutral Currents (FCNC). Therefore, since the FCNC processes are rather suppressed the possibility of MSSM enhancements should be very welcome, especially for the physics program at the LHC and perhaps also at a future linear collider LC. In the LHC, for example, the production of top quark pairs will be very high: $\sigma(t\bar{t}) = 800\ pb$ – roughly two orders of magnitude larger than that of the Tevatron II at $\sqrt{s} = 2\,TeV$. In the so-called low-luminosity phase ($10^{33}\,cm^{-2}s^{-1}$) of the LHC one expects about one $t\,\bar{t}$-pair per second, that is to say of the order of ten million $t\,\bar{t}$-pairs per year [7]. And this number will be augmented by one order of magnitude in the high-luminosity phase ($10^{34}\,cm^{-2}s^{-1}$). As for a future e^+e^- linear collider running at e.g. $\sqrt{s} = 500\ GeV$, one has a smaller cross-section $\sigma(t\bar{t}) = 650\ fb$ but a higher luminosity factor ranging from $5 \times 10^{33}\,cm^{-2}s^{-1}$ to $5 \times 10^{34}\,cm^{-2}s^{-1}$ [8] and of course a much cleaner environment. One thus expects that both the LHC and the LC will initially deliver datasets of order $10fb^{-1}$/year increasing to several $100\,fb^{-1}$/year in the high-luminosity phase. On the other hand, at the Tevatron II during the highest luminosity era (TeV33) one expects typical datasets of $30fb^{-1}$. It follows that if the branching ratios of the FCNC decays are augmented by extra contributions beyond the SM, one should be able to collect enough statistics (perhaps some few hundred to few thousand events) from the combined output of these machines enabling us to perform an efficient study of these rare decays.

We should immediately point out that, within the strict context of the SM, the possibility of detecting FCNC decays of the top quark is essentially hopeless. In particular, it has recently been recognized that the FCNC rate of the top quark decay into the SM Higgs boson ($t \to c\,H_{SM}$) is much smaller [9, 10] than originally thought [11]: It turns out that $BR(t \to c\,H_{SM}) = 1 \cdot 10^{-13} - 4 \cdot 10^{-15}$ $(M_Z \leq M_H \leq 2\ M_W)$ [9], which means that it is far out of the range to be covered by any presently conceivable high luminosity machine. On the other hand, the situation with the FCNC decays of the top quark into gauge bosons ($t \to c\,V$; $V \equiv \gamma, Z, g$) is not much more promising in the SM, the branching ratios being at most of order 10^{-12} for the photon, slightly above 10^{-13} for the Z-boson, and at most 10^{-10} for the gluon channel [11, 12]. Thus the highest SM rate, namely that of $t \to c\,g$, is still 5 (resp. 7) orders of magnitude below the feasible experimental possibilities at the LHC (resp. Tevatron II). Clearly, detection of FCNC decays of the top quark at visible levels (viz. $BR(t \to c\,X) \gtrsim 10^{-5} - 10^{-4}$) by any of the future high

[1]The corresponding study for general two-Higgs-doublet models (2HDM's) is also available in Ref. [3].

luminosity colliders would be instant evidence of new physics!

Therefore, one may judiciously ask whether extra virtual effects beyond the SM can help to bring the top quark FCNC decay ratios to within observable levels. For example, for the $t \to cV$ decays one finds, within the non-supersymmetric 2HDM's, that there can be significant enhancements[11, 13] which, however, turn out to be insufficient. A similar situation occurs in the more interesting case of the MSSM, where again in spite of the potential enhancements the electroweak gauge boson channels fall short to be detected [14]-[17]. Only the FCNC top quark decay in the gluon channel could be fairly sensitive to the SUSY corrections in non-negligible regions of the MSSM parameter space [14]-[17], a fact which we wish to revisit within our framework in order to compare with the more exceptional possibilities offered by the Higgs channels – on which we will mainly concentrate[2].

These Higgs channels comprise the FCNC top quark decays into the two CP-even ("scalar") states and the CP-odd ("pseudoscalar") state of the Higgs sector of the MSSM [19],

$$t \to c\,h \qquad (h = h^0, H^0, A^0). \tag{1}$$

Worth emphasizing is the fact that in the MSSM (in contrast to the SM or the unconstrained 2HDM) at least one of these decays (viz. $t \to c\,h^0$) is *always* possible, for in the MSSM there is an upper bound on the mass of the lightest CP-even Higgs boson, $M_{h^0} \lesssim 135\,GeV$[20]-[23], which is below the top quark mass. Moreover, for a sufficiently light pseudoscalar mass, $M_{A^0} < m_t$, all three decays (1) are in principle possible, if the SUSY masses are not that high so as to induce too large positive corrections to M_{H^0}.

As it is also the case with their charged-current counterpart mentioned in the beginning, these decays could be greatly enhanced in wide regions of the parameter space. Although some work already exists in the literature on FCNC decays of the top quark into Higgs bosons within the framework of the MSSM [24], we feel that it is still rather incomplete because it fails to include some of the most significant contributions and it does not make use of the one-loop Higgs mass relations of the MSSM [20]-[23]. These relations play an essential role in correlating the various quantum effects for the different channels (1) and are fundamental in establishing the aforementioned upper bound on the mass of the lightest supersymmetric Higgs particle. Therefore, our purpose is to go beyond those preliminary calculations and show, from a more rigorous and systematic treatment of the different kinds of quantum effects and of the MSSM parameter space, that the FCNC width of the top quark could in fact reach the experimentally visible level at the high-luminosity colliders [25].

The paper is organized as follows. In Sect. 2 we give the SUSY Lagrangian interactions relevant for the FCNC decays of the top quark. In Sect. 3 we report on the SUSY electroweak (SUSY-EW) and supersymmetric QCD (SUSY-QCD) one-loop contributions to the $t \to c\,h$ decays (1). In Sect. 4 we address the SUSY-QCD contributions to $t \to c\,g$ in our framework and compare with $t \to c\,h$. Finally, in Sect. 5 we further discuss our results and deliver our conclusions.

[2]For recent studies on FCNC top quark decays beyond the MSSM, see Ref. [18] and references therein.

2 Relevant interaction Lagrangians

The MSSM interaction Lagrangian involving fermions and $SU(3)_c \times SU(2)_L \times U(1)_Y$ gauge bosons is well-known, and will not be spelled out here in any detail[2, 6]. We will just focus on the relevant interaction pieces entering the main one-loop contributions to the Higgs channels (1).

To better present the analytic results of this computation we shall define first a notation that allows us to treat the three possible decays (1) in an unified way. We introduce a vector array of neutral Higgs fields

$$\Phi^0 = (H^0, h^0, A^0) \;, \tag{2}$$

and another one for the charged Higgs and Goldstone bosons

$$\Phi^+ = (H^+, G^+) \;. \tag{3}$$

Then the interaction Lagrangian of quarks with neutral and charged Higgs bosons in the MSSM can be written

$$\begin{aligned}
\mathcal{L}_{\Phi qq} \;=\; & -\frac{g\, m_u}{2M_W \sin\beta} \sum_{r=1,3} \Phi_r^0\, \overline{u}\, (K_r^{0u} P_L + (K_r^{0u})^* P_R)\, u \\
& -\frac{g\, m_d}{2M_W \cos\beta} \sum_{r=1,3} \Phi_r^0\, \bar{d}\, (K_r^{0d} P_L + (K_r^{0d})^* P_R)\, d \\
& +\frac{g}{\sqrt{2} M_W} V_{ud} \sum_{r=1,2} \left[\Phi_r^-\; \bar{d}\, (K_{rL}^{+ud} P_L + K_{rR}^{+ud} P_R)\, u + \text{ h.c.}\right] ,
\end{aligned} \tag{4}$$

with $P_{L,R} = (1/2)\,(1 \mp \gamma_5)$ the chirality projectors. We have defined the following sets of K-matrices: for the neutral Higgs sector

$$K_r^{0u} = \begin{pmatrix} \sin\alpha \\ \cos\alpha \\ i\cos\beta \end{pmatrix} \;,\quad K_r^{0d} = \begin{pmatrix} \cos\alpha \\ -\sin\alpha \\ i\sin\beta \end{pmatrix} \;, \tag{5}$$

and for the charged Higgs sector

$$K_{rL}^{+ud} = m_d \begin{pmatrix} \tan\beta \\ -1 \end{pmatrix} \;,\quad K_{rR}^{+ud} = m_u \begin{pmatrix} \cot\beta \\ 1 \end{pmatrix} \;. \tag{6}$$

In the above formula V_{ud} is the CKM matrix element (assumed to be the same as for the $W^\pm$ boson interactions with ordinary quarks).

The relevant Yukawa couplings involving charginos, quarks and squarks are contained in

$$\mathcal{L}_{u\,\tilde{d}\,\chi^+} = -g\, V_{ud}\, \tilde{d}_a^*\, \bar{\psi}_i^+ \left(A_{+ai}^{(d,u)}\, P_L + A_{-ai}^{(d,u)}\, P_R\right)\, u + \text{ h.c.} \;, \tag{7}$$

with u ($\tilde{d}$) up-type quarks (down-type squarks) of any generation, the coupling matrices being [26]

$$A_{+ai}^{(d,u)} = R_{1a}^{(d)*} V_{i1}^* - \lambda_d\, R_{2a}^{(d)*} V_{i2}^* \;,\; A_{-ai}^{(d,u)} = -R_{1a}^{(d)*} \lambda_u U_{i2} \;, \tag{8}$$

where

$$\lambda_u \equiv \frac{h_u}{g} = \frac{m_u}{\sqrt{2}\, M_W\, \sin\beta} \quad,\quad \lambda_b \equiv \frac{h_d}{g} = \frac{m_d}{\sqrt{2}\, M_W\, \cos\beta} \;, \tag{9}$$

are the up-like and down-like Yukawa couplings normalized with respect to the $SU(2)_L$ gauge coupling. Of fundamental importance for the SUSY-EW enhancement of our FCNC decays through these Yukawa couplings is the value of the parameter $\tan\beta = v_2/v_1$[19]. In the equations above $R^{(q)}$ is the 2×2 matrix that diagonalizes the squark mass squared matrix in chiral space through

$$\tilde{q}'_a = \sum_b R^{(q)}_{ab}\tilde{q}_b \ , \tag{10}$$

$\tilde{q}'_a$ being the weak-eigenstates and $\tilde{q}_a$ the mass-eigenstates.

Finally (regarding the EW part) we quote the interaction Lagrangian for triplet Higgs vertices in the MSSM[3]

$$\mathcal{L}_{\Phi\Phi\Phi} = -g\sum_{r,s,t} B_{rst}\,\Phi^+_r\,\Phi^-_s\,\Phi^0_t \ , \tag{11}$$

and the chargino couplings to neutral Higgs bosons

$$\mathcal{L}_{\chi^+\chi^+\Phi} = -g\sum_{r,i,j}\Phi^0_r\bar{\chi}^+_i(W^r_{ijL}\,P_L + W^r_{ijR}\,P_R)\chi^+_j \ . \tag{12}$$

In both cases we have encapsulated the remaining notation in two 3×3 matrices B_{rst} and W^r_{ij} whose explicit form can be identified from Ref. [19]. These matrices just give the corresponding Feynman rules (divided my $-ig$).

On the other hand, the necessary SUSY-QCD interactions (in the mass-eigenstate basis) for our FCNC decays are contained in the Lagrangian

$$\begin{aligned}\mathcal{L}_{\rm SUSY-QCD} &= -\frac{g_s}{\sqrt{2}}\,\bar{\psi}^{\tilde{g}}_c\,[R^*_{5\alpha}\,P_L - R^*_{6\alpha}\,P_R]\,\tilde{q}^*_{\alpha,i}\,\lambda^c_{ij}\,t_j \\ &- \frac{g_s}{\sqrt{2}}\,\bar{\psi}^{\tilde{g}}_c\,[R^*_{3\alpha}\,P_L - R^*_{4\alpha}\,P_R]\,\tilde{q}^*_{\alpha,i}\,\lambda^c_{ij}\,c_j \\ &- \frac{g_s}{\sqrt{2}}\,\bar{\psi}^{\tilde{g}}_c\,[R^*_{1\alpha}\,P_L - R^*_{2\alpha}\,P_R]\,\tilde{q}^*_{\alpha,i}\,\lambda^c_{ij}\,u_j + \text{ h.c.} \ ,\end{aligned} \tag{13}$$

where $\psi^{\tilde{g}}_c$ stands for the gluino spinor and λ^c are the $SU(3)_c$ Gell-Mann matrices. Moreover, the 6×6 rotation matrices $R^{(q)}$ generalize those in eq. (10) and are needed to diagonalize the squark mass matrices in (flavor)$\times$(chiral) space as follows[4]:

$$\begin{aligned}\tilde{q}'_\alpha &= \sum_\beta R^{(q)}_{\alpha\beta}\tilde{q}_\beta \ , \\ R^{(q)\dagger}\mathcal{M}^2_{\tilde{q}}R &= \mathcal{M}^2_{\tilde{q}D} = {\rm diag}\{m^2_{\tilde{q}_1},\ldots,m^2_{\tilde{q}_6}\} \quad (q\equiv u,\, d) \ ,\end{aligned} \tag{14}$$

where $\mathcal{M}^2_{(\tilde{u},\tilde{d})}$ is the 6×6 square mass matrix for squarks in the EW basis ($\tilde{q}'_\alpha$), with indices $\alpha = 1,2,3,\ldots,6 \equiv \tilde{u}_L,\tilde{u}_R,\tilde{c}_L,\ldots,\tilde{t}_R$ for up-type squarks, and a similar assignment for down-type squarks. However, in this study only up-type squarks are involved, so that we understand that the above diagonalizing matrices refer to them. The intergenerational mixing terms leading to gluino-mediated FCNC couplings lie in the off-diagonal entries of the mass matrices. However, in order to prevent the number of parameters from being

[3]Note that the elements B_{rs3} are complex and $B_{ss3} = 0$.

[4]First latin indices $(a,b,\ldots)$ refer to different squark states of the same flavor and take values $1,2$, with $m_{\tilde{q}_1} < m_{\tilde{q}_2}$ in the mass-eigenstate basis and $\tilde{q}'_{\{1,2\}} = \tilde{q}'_{\{L,R\}}$ in the weak-eigenstate basis. Latin indices $i,j,\ldots = 1,2$ refer to charginos. $r,s,\ldots$ refer to Higgs and Goldstone particles. Greek indices $\alpha,\beta,\ldots$ refer to squarks in the 6×6 (flavor)$\times$(chiral) space and take values $1,2,\ldots,6$, $m_{\tilde{q}_1} < m_{\tilde{q}_2} < \ldots < m_{\tilde{q}_6}$.

too large, we have allowed (symmetric) mixing mass terms only for the left-handed (LH) squarks. This simplification is often used in the MSSM and it is justified by Renormalization Group (RG) analysis [27]. Following this practice, we introduce intergenerational (that is to say, flavor mixing) coefficients δ_{ij} in the LL block of the mass matrix (namely the one involving only LH fields of any flavor) as follows:

$$(M^2_{LL})_{ij} = m^2_{ij} \equiv \delta_{ij}\, m_i\, m_j \quad (i \neq j) \;, \tag{15}$$

where m_i is the mass of the left-handed ith squark, and m^2_{ij} is the mixing mass matrix element between generations i and j. Therefore, if the coefficients δ_{ij} are non-vanishing, for some $i \neq j$, then the structure of the diagonalizing matrices $R^{(q)}$ defined above must necessarily lead to gluino-mediated tree-level FCNC between quarks and squarks in the SUSY-QCD Lagrangian (13). This scenario can be generalized if we further introduce FCNC interactions on the right-handed (RH) block of the mass matrix[28, 29] (see Sects. 4-5).

We note that the induced FCNC couplings in the SUSY-QCD Lagrangian (13) ultimately stem from the fact that the squark mass matrix in general need not to diagonalize with the same matrices as the quark mass matrix, i.e. the so-called misalignment of quark and squark mass matrices.

3 SUSY contributions to $t \to c\, h$

From the previous interaction Lagrangians, the computation of FCNC processes at one loop in a renormalizable theory is straightforward. In fact, renormalization of parameters and Green functions is not needed, unlike the usual flavor-conserving processes; one just computes the different diagrams that contribute to the process and the final result obtained after adding up all the amplitudes must be finite since no lowest order interaction could absorb the left over infinities.

For every decay process (1) it is convenient to define an "effective" interaction vertex

$$-i\,T \equiv -i\,g\;\overline{u}_c(p)\;(F_L\,P_L + F_R\,P_R)\;u_t(k)\;, \tag{16}$$

where F_L and F_R are form factors associated to each chirality projector. They follow from explicit calculation of vertices and mixed self-energies.

The one-loop graphs for the decays under study are depicted in Figs. 1, 2 and 3. On the one hand the contribution from the vertex diagrams (Figs. 1 and 3a) is obtained by direct calculation. On the other hand for the (mixed) self-energy diagrams (Cf. Figs. 2 and 3b) it is convenient to define (in analogy with the charged-current case [6]) the following structure:

$$\Sigma_{tc}(k) \equiv \not{k}\,\Sigma_L(k^2)\,P_L + \not{k}\,\Sigma_R(k^2)\,P_R + m_t\,\Big(\Sigma_{Ls}(k^2)\,P_L + \Sigma_{Rs}(k^2)\,P_R\Big)\;. \tag{17}$$

Here the m_t factor multiplying the scalar part is arbitrary and it is inserted there only to preserve the same dimensionality for the different Σ_i. From the Lagrangian interactions introduced in Sect. 1 we find that the effects of the mixed self-energy diagrams to the amplitude of $t \to c\;\Phi^0_r$ take on the following general form in terms of the various Σ_i:

$$-i\,T^r_{S_c} \;=\; \frac{-i\,g\,m_t}{2M_W \sin\beta}\,\frac{1}{m_c^2 - m_t^2}\,\bar{u}_c(p)\Big\{$$

$$
\begin{aligned}
& P_L\,K_r^{0t}\,\Big[m_c^2\Sigma_R(m_c^2)+m_c\,m_t\,\Big(\Sigma_{Rs}(m_c^2)+\Sigma_L(m_c^2)\Big)+m_t^2\,\Sigma_{Ls}(m_c^2)\Big]\\
& +P_R\,(K_r^{0t})^*\,[L\leftrightarrow R]\Big\}\,u_t(k)\ ,\\
-i\,T_{S_t}^r \ =\ & \frac{-i\,g\,m_c}{2M_W\sin\beta}\frac{m_t}{m_t^2-m_c^2}\bar{u}_c(p)\,\Big\{P_L\,K_r^{0c}\,\Big[m_t\,\Big(\Sigma_L(m_t^2)+\Sigma_{Rs}(m_t^2)\Big)\\
& +m_c\,\Big(\Sigma_R(m_t^2)+\Sigma_{Ls}(m_t^2)\Big)\Big]+P_R\,(K_r^{0c})^*\,[L\leftrightarrow R]\Big\}\,u_t(k)\ , \qquad (18)
\end{aligned}
$$

where we have called $T_{S_i}^r$ the amplitude corresponding to attaching the external rth Higgs particle line to the ith quark leg ($r=1,2,3$; $i=c,t$). From (18) the corresponding contribution to the form factors in eq. (16) is transparent.

3.1 SUSY-EW effects

We start by reporting on the SUSY-EW effects, which by definition include the sparticle contributions plus the Higgs-Goldstone boson diagrams computed in the Feynman gauge (Cf. Figs. 1 and 2). For the electroweak part we work in the so called Super-CKM basis, that is, we take the simplification that the squark mass matrix diagonalizes as the quark mass matrix, so that FCNC processes appear at one-loop only through the charged current interactions (from charged Higgs and charginos) and with the same mixing matrix elements as in the Standard Model (the CKM matrix). It means that for the electroweak effects we do not take into account the possible mismatch between the matrices diagonalizing the squark sector and those diagonalizing the quark sector as this would only result in a subleading additional correction.

Let us consider the computation of the contributions from diagrams in Figs. 1 and 2. The graphs in which FCNC are mediated by gauge bosons (W^+) have not been included since they are subdominant as compared to the leading effects from the Yukawa couplings of the top and (at large $\tan\beta$) bottom quarks. Still, the leading terms from longitudinal W^+ are taken into account through the inclusion of Goldstone bosons in the Feynman gauge.

The simplest SUSY-EW contributions are the self-energy diagrams (Fig. 2). They are obtained after substituting the following expressions into the generic eq. (18):

$$
\begin{aligned}
\Sigma_R(k^2)\Big|_{(a)} &= i\,g^2\,V_{td}\,V_{cd}\,A_{-ai}^{(d,c)}\,A_{-ai}^{(d,t)}\,B_1(k,M_i,m_{\tilde{d}_a})\ ,\\
\Sigma_L(k^2)\Big|_{(a)} &= i\,g^2\,V_{td}\,V_{cd}\,A_{+ai}^{(d,c)}\,A_{+ai}^{(d,t)}\,B_1(k,M_i,m_{\tilde{d}_a})\ ,\\
m_t\ \Sigma_{Rs}(k^2)\Big|_{(a)} &= i\,g^2\,M_i\,V_{td}\,V_{cd}\,A_{+ai}^{(d,c)}\,A_{-ai}^{(d,t)}\,B_0(k,M_i,m_{\tilde{d}_a})\ ,\\
m_t\ \Sigma_{Ls}(k^2)\Big|_{(a)} &= i\,g^2\,M_i\,V_{td}\,V_{cd}\,A_{-ai}^{(d,c)}\,A_{+ai}^{(d,t)}\,B_0(k,M_i,m_{\tilde{d}_a})\ ,\\
\Sigma_R(k^2)\Big|_{(b)} &= \frac{i\,g^2\,m_c\,m_t}{2\,M_W^2}V_{td}\,V_{cd}\,\Big[\cot^2\beta\ (B_0+B_1)\,(k,M_{H^\pm},m_d)\\
&\qquad +(B_0+B_1)\,(k,M_W,m_d)\Big]\ ,\\
\Sigma_L(k^2)\Big|_{(b)} &= \frac{i\,g^2\,m_d^2}{2\,M_W^2}V_{td}\,V_{cd}\,\Big[\tan^2\beta\ (B_0+B_1)\,(k,M_{H^\pm},m_d)\\
&\qquad +(B_0+B_1)\,(k,M_W,m_d)\Big]\ ,\\
m_t\ \Sigma_{Rs}(k^2)\Big|_{(b)} &= \frac{i\,g^2\,m_t\,m_d^2}{2\,M_W^2}V_{td}\,V_{cd}\,[B_0(k,M_{H^\pm},m_d)-B_0(k,M_W,m_d)]\ ,
\end{aligned}
$$

$$m_t\ \Sigma_{Ls}(k^2)\Big|_{(b)} \;=\; \frac{i\,g^2\,m_c\,m_d^2}{2\,M_W^2} V_{td}\,V_{cd}\,[B_0(k,M_{H^\pm},m_d)-B_0(k,M_W,m_d)]\ , \qquad (19)$$

where the two-point functions B_i are as in Ref.[6]. Of course in the above expressions we understand a sum over the free indices $a,i=1,2$ and over the three down-quark generations $(d=d,s,b)$.

The contribution to the form factors F_L and F_R in eq. (16) from SUSY-EW vertex diagrams is much more cumbersome. Diagrams (a) and (d) of Fig. 1 give a generic contribution of the form

$$\begin{aligned} F_L &= N_A\left[(C_{12}-C_{11})m_t\,A_R^{(1)}\,A_R^{(2)}-C_{12}\,m_c\,A_L^{(1)}\,A_L^{(2)}+C_0\,m_A\,A_R^{(1)}\,A_L^{(2)}\right]\ , \\ F_R &= F_L\,(A_L^{(*)}\leftrightarrow A_R^{(*)})\ , \end{aligned} \qquad (20)$$

whereas diagrams (b) and (c) have the general structure

$$\begin{aligned} F_L = N_D\ \Big[&C_0\,(D_L^{(1)}\,D_L^{(2)}\,D_R^{(3)}\,m_c\,m_t+D_L^{(1)}\,D_L^{(2)}\,D_L^{(3)}\,m_c\,m_{D1} \\ &+D_R^{(1)}\,D_L^{(2)}\,D_R^{(3)}\,m_t\,m_{D2}+D_R^{(1)}\,D_L^{(2)}\,D_L^{(3)}\,m_{D1}\,m_{D2}) \\ &+C_{12}\,m_c\,(D_R^{(1)}\,D_R^{(2)}\,D_L^{(3)}\,m_c+D_L^{(1)}\,D_L^{(2)}\,D_R^{(3)}\,m_t \\ &+D_L^{(1)}\,D_L^{(2)}\,D_L^{(3)}\,m_{D1}+D_L^{(1)}\,D_R^{(2)}\,D_L^{(3)}\,m_{D2}) \\ &+(C_{11}-C_{12})\,m_t\,(D_L^{(1)}\,D_L^{(2)}\,D_R^{(3)}\,m_c+D_R^{(1)}\,D_R^{(2)}\,D_L^{(3)}\,m_t \\ &+D_R^{(1)}\,D_R^{(2)}\,D_R^{(3)}\,m_{D1}+D_R^{(1)}\,D_L^{(2)}\,D_R^{(3)}\,m_{D2})+\tilde{C}_0\,D_R^{(1)}\,D_R^{(2)}\,D_L^{(3)}\Big]\ , \\ F_R = F_L(&D_L^{(*)}\leftrightarrow D_R^{(*)})\ , \end{aligned} \qquad (21)$$

where the three-point functions C_i and C_{ij} are as in Ref.[1, 6].

Specifically, each vertex diagram of Fig. 1 contributes the following to the process $t\to c\ \Phi_r^0$:

- Diagram (a); make the following substitutions in eq. (20):

$$\begin{aligned} &A_L^{(1)}=A_{+bi}^{(d,c)}\ ,\ A_R^{(1)}=A_{-bi}^{(d,c)}\ ,\ A_L^{(2)}=A_{+ai}^{(d,t)}\ ,\ A_R^{(2)}=A_{-ai}^{(d,t)}\ , \\ &m_A=M_i\ ,\ N_A=i\,g^2V_{td}V_{cd}R_{ea}^{(d)}\,(R_{fb}^{(d)})^*\,G_{fe}^r\ , \end{aligned}$$

  where G_{fe}^r is the well-known Feynman rule [19] for the vertex $\Phi_r^0\tilde{d}'_f\,\tilde{d}'^*_e$ divided by $-ig$, in the electroweak-eigenstate basis[5]. In this diagram the various three-point functions on (20) must be evaluated with arguments

$$C_*=C_*(k,-p',M_i,m_{\tilde{d}_a},m_{\tilde{d}_b})\ .$$

  The convention for the momenta can be seen in Fig. 1a.

- Diagram (b); make the following substitutions in eq. (21):

$$\begin{aligned} &D_L^{(1)}=A_{+aj}^{(d,c)}\ ,\ D_R^{(1)}=A_{-aj}^{(d,c)}\ ,\ D_L^{(2)}=W_{ijL}^r\ ,\ D_R^{(2)}=W_{ijR}^r\ , \\ &D_L^{(3)}=A_{+ai}^{(d,t)}\ ,\ D_R^{(3)}=A_{-ai}^{(d,t)}\ , \\ &m_{D1}=M_i\ ,\ m_{D2}=M_j\ ,\ N_D=i\,g^2\,V_{td}\,V_{cd}\ , \\ &C_*=C_*(k,-p',m_{\tilde{d}_a},M_i,M_j)\ , \end{aligned}$$

[5] We recall that our sign convention [1, 6, 26] for the μ parameter is opposite to that of [19].

- Diagram (c); substitute in eq. (21):

$$\begin{aligned}
&D_L^{(1)} = K_{sL}^{+cd}\ ,\ D_R^{(1)} = K_{sR}^{+cd}\ ,\ D_L^{(2)} = K_s^{0d}\ ,\ D_R^{(2)} = (K_s^{0d})^*\ ,\\
&D_L^{(3)} = K_{sR}^{+td}\ ,\ D_R^{(3)} = K_{sR}^{+td}\ ,\\
&m_{D1} = m_{D2} = m_b\ ,\ N_D = i\frac{g^2\, m_d}{4M_W^3\,\cos\beta} V_{td}V_{cd}\ ,\\
&C_* = C_*(k, -p', m_{\Phi_s^+}, m_d, m_d)\ ,
\end{aligned}$$

- Diagram (d); substitute in eq. (20):

$$\begin{aligned}
&A_L^{(1)} = K_{vL}^{+cd}\ ,\ A_R^{(1)} = K_{vR}^{+cd}\ ,\ A_L^{(2)} = K_{sL}^{+td}\ ,\ A_R^{(2)} = K_{sR}^{+td}\ ,\\
&m_A = m_d\ ,\ N_A = i\frac{g^2}{2\,M_W^2}\, B_{svr}\, V_{td}\, V_{cd}\ ,\\
&C_* = C_*(k, -p', m_d, m_{\Phi_s^+}, m_{\Phi_v^+})\ .
\end{aligned}$$

As can be noted from the above expressions, the form factors induced by Higgs mediated diagrams – see Figs. 1c and d – have the property $F_L = F_R$ for H^0 and h^0, and $F_L = -F_R$ for A^0.

We have performed the usual checks of the computation, in particular we find that the form factors F_L and F_R are free of divergences before adding up the three quark generations, both analytically and numerically in the implementation of the code.

3.2 SUSY-QCD effects

Using the Lagrangians (4) and (13) one can find the SUSY-QCD one-loop contributions to the processes under study. They are much more simple than the electroweak ones. The Feynman diagrams are depicted in Figs. 3a and b. The one-loop mixed self-energy in Fig. 3b is determined from

$$\begin{aligned}
\Sigma_L(k^2) &= -i\,2\,\pi\,\alpha_s\,C_F\,R_{3\alpha}\,R_{5\alpha}^*\,B_1(-k, m_{\tilde g}, m_{\tilde u_\alpha})\ ,\\
\Sigma_R(k^2) &= -i\,2\,\pi\,\alpha_s\,C_F\,R_{4\alpha}\,R_{6\alpha}^*\,B_1(-k, m_{\tilde g}, m_{\tilde u_\alpha})\ ,\\
m_t\,\Sigma_{Ls}(k^2) &= -i\,2\,\pi\,\alpha_s\,C_F\,m_{\tilde g}\,R_{4\alpha}\,R_{5\alpha}^*\,B_0(-k, m_{\tilde g}, m_{\tilde u_\alpha})\ ,\\
m_t\,\Sigma_{Rs}(k^2) &= -i\,2\,\pi\,\alpha_s\,C_F\,m_{\tilde g}\,R_{3\alpha}\,R_{6\alpha}^*\,B_0(-k, m_{\tilde g}, m_{\tilde u_\alpha})\ ,
\end{aligned}\tag{22}$$

where $C_F = (N_c^2-1)/2N_c = 4/3$ is the quadratic Casimir invariant of the fundamental representation of $SU(3)_c$.

Finally, the SUSY-QCD vertex contributions to the form factors (16) follow from Fig. 3a, and read

$$\begin{aligned}
F_L &= N\,[m_t\,R_{4\beta}\,R_{6\alpha}^*\,(C_{11}-C_{12}) + m_c\,R_{3\beta}\,R_{5\alpha}^*\,C_{12} + m_{\tilde g}\,R_{4\beta}\,R_{5\alpha}^* C_0]\ ,\\
F_R &= F_L\,(3\leftrightarrow 4\ ,\ 5\leftrightarrow 6)\ ,\\
N &= i\,8\,\pi\,\alpha_s\,C_F\,R_{\gamma\beta}^*\,G_{\gamma\delta}^r\,R_{\delta\alpha}\ ,\\
C_* &= C_*(-k, p', m_{\tilde g}, m_{\tilde u_\alpha}, m_{\tilde u_\beta})\ ,
\end{aligned}\tag{23}$$

where $G_{\gamma\delta}^r$ is the well-known Feynman rule (divided by $-ig$) [19] for the vertex $\Phi_r^0\tilde u_\gamma'\tilde u_\delta'^*$ in the electroweak-eigenstate basis. From these expressions it should be clear that if the up-type squarks would be degenerate, then by the unitarity of the R-matrices the gluino-mediated FCNC effects would vanish (GIM mechanism). We have used this analytical property as an additional check of our numerical code.

4 Numerical Analysis of $t \to c\, h$

After squaring the matrix element (16), and multiplying by the phase space factor, one obtains the decay width of $t \to c\, h$,

$$\begin{aligned}\Gamma(t \to c\, h) &= \frac{g^2}{32\,\pi\, {m_t}^3}\lambda^{1/2}(m_t^2, m_h^2, m_c^2) \\ &\times \left[(m_t^2 + m_c^2 - m_h^2)(|F_L|^2 + |F_R|^2) + 2\, m_t\, m_c\,(F_L\, F_R^* + F_L^*\, F_R)\right]\ ,\end{aligned} \tag{24}$$

with $\lambda(x^2, y^2, z^2) = (x^2-(y+z)^2)(x^2-(y-z)^2)$ the usual Källen function. It is conventional to define the ratio

$$B(t \to c\, h) \equiv \frac{\Gamma(t \to c\, h)}{\Gamma(t \to b\, W^+)}\,, \tag{25}$$

which will be the main object of our numerical study.

This ratio is not the total branching fraction $BR(t \to c\, h)$ of the decay mode, as there are many other channels that should be added up to the denominator of (25) in the MSSM, if kinematically allowed, such as the two and three body decays of the top quark into SUSY particles, and also the charged Higgs decay channel $t \to H^+\, b$ [1, 26]. For the mass spectrum used in our numerical analysis the former decays are phase space closed, whereas the latter could have a sizeable branching ratio. However, for better comparison with previous analyses of FCNC top quark decays [9]-[17], the fiducial quantity (25) should suffice to assess the experimental viability of the FCNC decays under consideration.

In the following we will analyze the numerical contributions to (25) from the SUSY-EW and SUSY-QCD sectors, in a sparticle mass model motivated by model building and RG analysis. However, we do not restrict ourselves to the spectrum of specific SUSY-GUT models – such as SUGRA or constrained MSSM models[2, 30]. Furthermore, as announced in the beginning, all over our numerical analysis we use the full structure of the one-loop relations for the parameters in the Higgs sector of the MSSM [21].

We start with the EW effects. Although we have generally scanned the MSSM parameter space up to $1\, TeV$ level, the following input set has been chosen where the individual parameters have to be fixed at particular values to illustrate our results (as in Fig. 4):

$$\begin{aligned}&\tan\beta = 35\ ,\ \mu = -500\, GeV\ ,\ M = 150\, GeV\ ,\ M_{A^0} = 100\, GeV\ , \\ &m_{\tilde{t}_1} = 150\, GeV\ ,\ m_{\tilde{b}_1} = m_{\tilde{q}} = 200\, GeV\ ,\ A_t = A_q = 300\, GeV\ ,\ A_b = -300\, GeV\ .\end{aligned} \tag{26}$$

We have taken the third generation quark masses as $m_t = 175\, GeV$ and $m_b = 5\, GeV$. In the previous equation $m_{\tilde{t}_1}, m_{\tilde{b}_1}$ are the lightest $\tilde{t}$ and $\tilde{b}$ mass, and all the masses are above present experimental bounds [31]. However, we have chosen a SUSY mass spectrum around $200\, GeV$, which is not too light, so the results will not be artificially optimized. We have also checked that all through our numerical analysis other bounds on experimental parameters (such as $\delta\rho$) are fulfilled.

We have found that the contributions to the form factors of (16) are of the same order for the chargino (Figs. 1a,b and 2a) and Higgs particles [32] (Figs. 1c,d and 2b) –not included in previous analyses [24]. It turns out that they can be either of the same sign, or of opposite sign. The chosen negative value for A_b is to make the two contributions of the same sign. In both cases $F_R \gg F_L$. This can be easily understood by looking at the interaction vertices involving (charged)Higgs-bottom-charm [19] and chargino-sbottom-charm, where the latter can be tracked down from the explicit structure of the Lagrangian (7). In both of them the contribution to the right-handed form factor will be enhanced by the Yukawa coupling of the bottom quark, whereas the charm Yukawa coupling contributes to the left-handed form factor. We have checked that the inclusion of the first two generations of quarks and squarks only has an effect of a few percent on the total result.

In Fig. 4 we can see the evolution of the ratio (25) with various parameters of the MSSM by taking into account only the electroweak contributions. The growing of the width with $\tan\beta$ (Cf. Fig. 4a) makes evident that the bottom quark Yukawa coupling plays a central role in these contributions. The evolution with the trilinear coupling A_b –the main parameter that appears in the interaction vertex $\tilde{b}_L\,\tilde{b}_R\,h$– displayed in Fig. 4b shows that this parameter can enhance the width by some orders of magnitude. On the other hand the evolution with he higgsino mass parameter μ (Cf. Fig. 4c) is comparatively mild in the region away from the origin $\mu = 0$. The shaded region in Fig. 4c, centered at the origin, is ruled out by present LEP bounds on chargino masses [31]. As the dependence of the rate (25) on the $SU(2)_L$ gaugino mass M is essentially flat (not shown), these LEP bounds effectively translate in our case into excluding $\mu \lesssim 90\,GeV$. The various spikes in these figures reflect the points where the overall numerical contribution from the form factors (vertex plus self-energy) cancels out and even changes sign. The actual point where this cancellation occurs depends on the particular choice of the parameters.

The fact that in all these figures the ratio (25) is smaller for the heaviest scalar Higgs (H^0) is not due to the smaller phase space factor, but to the smallness of the form factors. We can see in Fig. 4d that in fact $B(t \to c\,H^0)$ grows with the A^0 (and thus the H^0) mass, until the phase space begins to close.

We conclude that a typical value of the ratio (25), at large $30 \lesssim \tan\beta \lesssim 50$ and for a SUSY spectrum around $200\,GeV$, reads roughly

$$B^{\mathrm{SUSY-EW}}(t \to c\,h) \simeq 10^{-8} \quad , \tag{27}$$

provided $M_A < 120 - 130\,GeV$. This is larger than the previous reported ratios [24] by 2 orders of magnitude, specially in the A^0 channel, and it is at least 5 orders of magnitude larger than the SM rate $B(t \to c\,H_{SM})$ [9, 10]. In fact, this feature can be explicitly checked in our framework in the limit $M_{A^0} \to \infty$ in which the CP-even Higgs boson h^0 behaves like the SM Higgs boson H_{SM}. This is already seen in part in Fig. 4d. By further sending the SUSY masses to infinity we indeed recover a very poor FCNC rate for $h^0 \sim H_{SM}$ which goes down 10^{-13}[9, 10].

Turning now to the analysis of the SUSY-QCD effects, it is clear that they hinge to a great extent on the values of the flavor mixing coefficients δ_{ij}. The latter are constrained by low-energy data on FCNC. The bounds have been computed using some approximations, so they must be taken as order of magnitude limits rather than as accurate numbers. They read as follows [28, 29]:

$$\begin{aligned}
|\delta_{12}| &< .1\,\sqrt{m_{\tilde{u}}\,m_{\tilde{c}}}/500\,GeV \ , \\
|\delta_{13}| &< .098\,\sqrt{m_{\tilde{u}}\,m_{\tilde{t}}}/500\,GeV \ , \\
|\delta_{23}| &< 8.2\,m_{\tilde{c}}\,m_{\tilde{t}}/(500\,GeV)^2 \ .
\end{aligned} \tag{28}$$

In using these bounds we make use of $SU(2)$ gauge invariance to transfer the experimental information known from the down-quark sector (for example from $BR(b \to s\,\gamma)$, where the bound on δ_{23} is obtained) to the up-quark sector. It means that after soft SUSY breaking, but before SSB, the LL blocks of the up-squark and down-squark mass matrices must satisfy the following relation [29]

$$(M^2_{\tilde{U}})_{LL} = K\,(M^2_{\tilde{D}})_{LL}\,K^\dagger\;, \tag{29}$$

where K is the Cabibbo-Kobayashi-Maskawa matrix. Thus if $M^2_{\tilde{D}}$ is parametrized as in eq. (15), then $(M^2_{\tilde{U}})_{LL}$ inherits a similar form with a new set of mixing coefficients δ_{ij}which differ from the previous ones by factors of $\mathcal{O}(1)$.

We use the same input parameters as in the electroweak contributions (26), plus the specific parameters of the SUSY-QCD sector, namely the gluino mass $m_{\tilde{g}}$ and the mixing coefficients δ_{ij}, as follows:

$$\begin{aligned} m_{\tilde{g}} &= 200\;GeV\;, \\ \delta &= \begin{pmatrix} 0 & 0.03 & 0.03 \\ 0.03 & 0 & 0.4 \\ 0.03 & 0.4 & 0 \end{pmatrix}\;. \end{aligned} \tag{30}$$

As for the strong coupling constant we have used the value $\alpha_s(m_t^2) = 0.11$. A comment is in order for the present set of inputs: we have introduced in (26) the lightest stop mass as an input, and this stop is mostly a $\tilde{t}_R$. However, in this new parametrization we introduce this mass as the lightest $\tilde{u}_\alpha$ mass, which again will be mostly a $\tilde{t}_R$. Notice furthermore that the chosen entries in the mixing matrix (30) are moderate in the sense that they do not saturate the permissible upper limits (28). Here we are using the additional constraint that the squark masses (which are obviously affected by the values of the parameters δ_{ij}) cannot be too light. As mentioned above, although we use a fixed "typical" choice of inputs, a systematic scanning has been performed over the parameter space. In particular, the maximum values for the rates (to be compared with the typical ones) have also been pinned down (see later on).

In analyzing the SUSY-QCD effects we find that again the largest contribution comes from the right-handed form factor in eq. (16), but this is only because up to now we have chosen not to introduce mixing between right-handed squarks. We have plotted the evolution of the ratio (25) with some parameters of the MSSM in Fig. 5. As it reads off eq. (30) the most relevant parameter in the SUSY-QCD analysis is the mixing coefficient between the 2nd and 3rd generation of LH squarks, which is the less restricted one of the three in eq. (28). In Fig. 5a it is shown that by changing δ_{23} by 3 orders of magnitude the ratio (25) increases by 6 orders of magnitude! – a fact that can be traced to the quadratic dependence on the mixing coefficient. Worth noticing in Fig. 5b is the μ parameter dependence of the SUSY-QCD effects, which enters through the $\tilde{q}_L\tilde{q}_R h$ coupling. The ratio (25) can be pushed up to values of 10^{-5} irrespective of the sign of μ. Again the central region of μ is excluded by present LEP bounds on the chargino masses.

The evolution with the gluino mass (Cf. Fig. 5c) is asymptotically quite stable, showing a slow decoupling. Thus, even for gluinos as heavy as $500\,GeV$ the rate for the top quark decay into the lightest CP-even Higgs boson ($t \to c\,h^0$) can stay above 10^{-5}. Finally in Fig. 5d we have plotted the evolution with the pseudoscalar Higgs mass. It is seen a behavior similar to the EW case (Cf. Fig. 4d) although scaled up a factor $10^2 - 10^3$. Obviously, the one-loop Higgs mass relations play an essential role here (missed in [24]) in that the h^0 is bound to have a mass (below $\sim 135\,GeV$) which is higher than in the tree-level case (below M_Z). Still the asymptotic behavior of $B(t \to c\,h^0)$ versus M_{A^0} is sustained a long while around 10^{-6} for a SUSY spectrum of a few hundred GeV.

Figs. 6a and b display the change of (25) with the lightest stop and sbottom masses within the allowed region. It is clear that $m_{\tilde{t}_1}$ plays an important role, which is due to the fact that by changing this parameter one is also changing the value of the mixing angle between the LH and RH stops. On the other hand the actual value of $m_{\tilde{b}_1}$ is seen not to be that important in the A^0 and h^0 channels.

In Fig. 6c we plot the ratio (25) versus $\tan\beta$. We see that the evolution of the SUSY-QCD contributions as a function of $\tan\beta$ is quite stable for the h^0 and A^0 channels, and so it does not matter much, in the SUSY-QCD case, whether we are in the low or in the high $\tan\beta$ region. The pronounced downwards spike around $\tan\beta \simeq 10$ for the H^0 channel is due to the change of sign of the form factor.

For completeness we have explicitly probed the impact on the FCNC rates in the presence of intergenerational mass-mixing terms in the right-handed sector of the model. In order to maintain the number of parameters under control we have set $(\delta_{ij})_{RR} = (\delta_{ij})_{LL}$. We find that the inclusion of the additional mixing coefficients does increase the FCNC rate, but we do not plot the result since it just amounts to a total contribution which is at most twice the old result with $(\delta_{ij})_{RR} = 0$. And this feature holds for any set of input parameters (26,30). Therefore, we conclude that the old coefficients $(\delta_{ij})_{LL}$ alone –the only ones that are naturally generated within RG-based models [27] – already bring about the bulk of the FCNC rates (25).

We wish to emphasize that although we have used a common subset of inputs –see eq. (26)– to compute the SUSY-EW and the SUSY-QCD loops, the enhancement sources for the two types of contributions are entirely different. Thus, whereas the SUSY-EW effects are much sensitive to extreme values of the parameter $\tan\beta$ through the Yukawa couplings (9), the SUSY-QCD effects (which are the leading ones in our calculation) are not particularly sensitive to $\tan\beta$, as confirmed in Fig. 6c. Instead, they are basically dependent on the experimentally allowed values of the flavor mixing coefficients (15), as it is plain in Fig. 5a.

From the previous numerical analysis we confirm that the preliminary MSSM treatment of the FCNC decay of the top quark into Higgs bosons [24] was fairly incomplete since important effects from Higgs particles in the loops were not included, and moreover the $\tilde{q}_L\,\tilde{q}_R\,h$ vertices were not taken into account. As a result the potentially large contributions coming from the trilinear soft SUSY-breaking terms $A_{t,b}$, and from the higgsino mass parameter μ were missed. Moreover, the pattern of quantum effects in the three Higgs channels is affected in an essential way by the one-loop Higgs mass relations of the MSSM. From our rigorous computation we have been able to show that $B(t \to c\,h)$ in the MSSM can typically be of order 10^{-8} for the electroweak contributions, and reach 10^{-5} for the QCD contributions. In some of the channels this amounts to having rates that are one to two orders of magnitude larger than previous estimates. For an assessment of the impact of these results on experimental searches, and a discussion of the maximum attainable rates, see Sect. 6.

5 The decay $t \to c\, g$

We have already mentioned that the FCNC decays of the top quark into gauge bosons, $t \to c\ V$, may receive important contributions from SUSY physics, and this has been confirmed by explicit calculations in the literature [14]-[17]. In particular, the situation with the decays $t \to c\,V$ into electroweak gauge bosons $V = \gamma, Z$ is that, in spite of the SUSY enhancements, the final rates are far insufficient to be seen, except for very especial circumstances associated to the possibility of wave-function threshold effects [16]. These effects, however, are "point-like coincidences", so to speak, which we deem to be very unlikely. Indeed, a similar situation occurs e.g. when computing the SUSY corrections to the conventional decay of the top quark, $t \to W^+ b$ [6]. Also in this case there are particular combinations of sparticle masses which fall within the (very) narrow range where wave-function threshold enhancements occur[6]. To be sure, this circumstance should be considered exceptional and so the fairest conclusion ought rather to be that the SUSY effects on $t \to W^+ b$ are generally small, and similarly that the SUSY rates for the FCNC decays $t \to c\,(\gamma, Z)$ are far below the experimental possibilities.

In the specific case of the gluon channel $t \to c\ g$ one could also argue that it could be enhanced by threshold effects, only if the top quark, gluino and stop masses turned out to satisfy the peculiar relation $m_t \simeq m_{\tilde{t}} + m_{\tilde{g}}$. Nonetheless a relation like this is not only contrived, but it is already ruled out by the current bounds on gluino and stop masses [31]: $m_{\tilde{g}} > 180\ GeV$, $m_{\tilde{t}_1} > 80\ GeV$. Fortunately, in contrast to the electroweak gauge boson channels just mentioned, alternative important corrections to $t \to c\ g$ are possible from gluino-mediated FCNC loops. This subject has recently been addressed in Ref. [17], but due to discrepancies of this reference with previous calculations by the authors of Refs.[14, 15] we wish to reanalyze this decay in our framework. In this way we hope to further clarify the situation and at the same time to use $t \to c\ g$ as a fiducial observable with which to better compare the results that we find for the $t \to c\ h$ channels within one and the same set of assumptions.

The diagrams contributing to $t \to c\ g$ are similar to those in Figs. 1a,c and 3 after replacing the Higgs boson h with the gluon g. The corresponding SM contribution involves the W gauge boson and the bottom quark flowing in the loop. However, in the conditions of the foregoing study of $t \to c\ h$, we have seen that the set of electroweak diagrams in Figs. 1-2 furnish in general a negligible contribution as compared to the gluino-mediated contributions in Fig. 3 – and we find that this does not change for the decay $t \to c\ g$. Therefore, we only report on the corresponding SUSY-QCD effects.

A crucial point in computing this type of effects in the case of $t \to c\,h$ was to realize that there are diagrams in the electroweak eigenstate-basis with an helicity flip at the gluino line. As a result the decay $t \to c\ h$ received contributions "proportional" to the gluino mass –Cf. eq. (23). These terms cause the corresponding decay rate to fall off very slowly with $m_{\tilde{g}}$, and they even produce a local maximum with respect to this parameter (recall Fig. 5c). Similarly, it turns out that the decay $t \to c\ g$ can also have this kind of enhancements, although from a slightly different origin (see below). This fact, with which we agree with the recent calculation of Ref.[17], was missed in Refs. [14, 15] and it led them to speculate on the existence of additional gluino-mediated FCNC interactions in the RH sector in order to reach higher rates. Although these additional terms are possible, in principle, they are unnatural in a RG-based framework; and what is more,

[6]See Ref. [6] for details, and in particular Figs. 6, 7 and 8 of that reference.

they are actually unnecessary to potentially achieve the desired enhancements.

The analytical calculations for $t \to c\, g$ are similar to those for $t \to c\, h$, and so we just report on the numerical analysis, which we present in Figs. 7-9. In all these figures we exhibit the evolution of the ratio $B(t \to c\, g)$ – defined as in eq. (25) with g replacing h – for two different scenarios, namely, when only mixing between LH squarks is allowed (solid lines), and when mixing mass terms are allowed also in the RH squark sector (dashed lines). If one sticks to the more conservative FCNC gluino-mediated interactions in the pure LH sector, we see that one may reach important enhancements which can bring $B(t \to c\, g)$ up to 10^{-6}-10^{-5} for allowed sparticle masses[7]. However, as in the $t \to c\, h$ case, we find that the inclusion of FCNC in the RH sector do not modify the order of magnitude of the results; in fact the RH interactions only enhance the previous result by at most a factor of 2.

In the calculation, when including the RH terms, we have set $(\delta_{ij})_{RR} = (\delta_{ij})_{LL}$ and used the fact that the bounds on $(\delta_{ij})_{LL}$ are interwoven with the bounds on the squark masses [29] as dictated by eq. (15), similarly as we did in our analysis of the $t \to c\, h$ decays in Sect. 3.

In Fig. 7 we display the evolution of $B(t \to c\, g)$ as a function of the mixing parameter δ_{23} and the gluino mass $m_{\tilde{g}}$. We see that $B(t \to c\, g)$ is also proportional to $(\delta_{23})^2$ as $B(t \to c\, h)$. The evolution with the gluino mass also exhibits a local maximum, characteristic of the terms "proportional" to $m_{\tilde{g}}$ that are triggered by the helicity flip in the gluino line. As we said before, this flip occurs even if we only allow intergenerational mass-mixing terms in the LL block of the mass matrix – a feature which was completely overlooked in Ref.[15]. The origin of the flip in the electroweak-eigenstate basis is as follows. In the one-loop vertex diagram there exists a FCNC gluino interaction with the LH charm quark and the LH stop, where the latter stems from a RH stop that has mutated (through a mixed propagator) into a LH state. This situation is favorable because of large LR mixing in the stop sector. Schematically, one can think in terms of the following picture: from the gluon vertex in the loop there emerges a $\tilde{t}_R$ that subsequently undergoes the series of transitions $\tilde{t}_R \to \tilde{t}_L \to c_L$ [8]. As the structure of this loop enforces a mass insertion in the gluino propagator, it leads to an enhancement of $B(t \to c\, g)$ which nevertheless falls off with the gluino mass much faster than in the $B(t \to c\, h)$ case (Cf. Fig. 5c).

The evolution with the electroweak parameters $\tan\beta$ and μ is presented in Fig. 8. In this process they only enter as inputs in the squark mass matrix, but not in the couplings, so the dependence of $B(t \to c\, g)$ on them is rather mild. In the presence of mixing in both the LH and RH sectors, the physical squarks masses are smaller than the corresponding ones with mixing only in the LH sector. Eventually these particles can be lighter than present bounds, thus the parameter space is further constrained. This is shown in Fig. 8 where the dashed lines (corresponding to $\delta_{LL} = \delta_{RR}$) are cut off at points in which the present bounds on squarks masses would be violated. Finally, we report in Fig. 9 on the evolution with the lightest stop mass and the soft SUSY-breaking trilinear coupling A_t. The shaded region in Fig. 9b is excluded as it incompatible with our choice of parameters,

[7]When comparing with Ref. [17], in the unconstrained MSSM case, we point out that our rates are smaller only because we use an updated (larger) value of the gluino mass and also a larger value for the lightest stop mass – see eq. (26)– which is the most sensitive one.

[8]The difference with the $t \to c\, h$ case lies in the fact that the first transition $\tilde{t}_R \to \tilde{t}_L$ is already possible at the Higgs vertex $\tilde{t}_L\, \tilde{t}_R\, h$ in the loop, but it cannot take place at the gluon vertex.

and the various lines end up where the large mixing would induce too light squark masses. The rate is seen to be sensitive to both parameters $m_{\tilde{t}_1}$ and A_t, but the actually permitted region for the latter is quite narrow.

To summarize, upon comparing the decay $t \to c\, g$ with the relevant decays $t \to c\, h$ under study we find that the latter can be relatively very important, and most likely they are the dominant FCNC top quark decays in the MSSM. As a matter of fact, whereas the critical level 10^{-5} is never surpassed by the gluon channel – even with LH+RH effects and for sparticle masses within the current limits–, the $t \to c\, h^0$ and $t \to c\, A^0$ modes, instead, may well crossover the visible level already with the more conventional LH contributions. The maximum values for all these decays are discussed in the next section, where we also present our conclusions.

6 Discussion and conclusions

We have studied the SUSY-EW and SUSY-QCD contributions to the leading FCNC top quark decays. We have mainly concentrated on the top quark FCNC decays into the Higgs bosons of the MSSM, namely $t \to c\, h$ $(h = h^0, H^0, A^0)$, using a mass spectrum motivated, but not fully restricted, by model building and Renormalization Group Equations. And we have found that a full treatment of the SUSY-QCD contributions may greatly enhance the FCNC width by some orders of magnitude with respect to the FCNC decay rates into gauge bosons $t \to c\, V$ $(V \equiv \gamma, Z, g)$. Due to the crucial role played by the SUSY-QCD effects, we have reconsidered the FCNC decay into gluons, $t \to c\, g$, which is the most promising one among the FCNC top quark decays into gauge bosons. And we have shown that under similar assumptions of gluino-mediated FCNC couplings in the LH sector, it could be enhanced up to near the visible level, but below the rates of the Higgs channels. The additional RH interactions, if present at all, could produce a further increase of the rates, but it just amounts a factor of 2 at most. The remaining gauge boson channels give maximum rates in the MSSM that are far below experimental possibilities, except in highly unlikely circumstances.

With a SUSY mass spectrum around $200\, GeV$, which is above the current absolute LEP bounds [31], the different contributions to the Higgs channels are typically of the order

$$\begin{aligned} B^{\rm SUSY-EW}(t \to c\, h) &\simeq 10^{-8}\ , \\ B^{\rm SUSY-QCD}(t \to c\, h) &\simeq 10^{-5}\ . \end{aligned} \tag{31}$$

However, by stretching out a bit more the range of parameters one can reach (for some of the decays)

$$\begin{aligned} B^{\rm SUSY-EW}(t \to c\, h) &\simeq 1 \times 10^{-6}\ , \\ B^{\rm SUSY-QCD}(t \to c\, h) &\simeq 5 \times 10^{-4}. \end{aligned} \tag{32}$$

The difference of at least two orders of magnitude between the SUSY-EW and SUSY-QCD contributions makes unnecessary to compute the interference terms between the two sets of amplitudes, but if the limits on δ_{23} (eq. (28)) become eventually more restrictive then they should be taken into account.

We have obtained the maximum rates (32) from a general search in the MSSM parameter space within the $1\, TeV$ mass region. In Fig. 10 we present the maximum values that can be reached by $B(t \to c\,X)$ for each of the processes presented. In Figs. 10a and b we show the maximized $B(t \to c\,h)$ as a function of the pseudoscalar Higgs boson mass by taking into account only the SUSY-EW contributions and the SUSY-QCD contributions respectively. We have performed a systematic scanning of the parameter space of the MSSM, with the various masses constrained between the present exclusion bounds and the $1\,TeV$ upper bound, and using the other bounds from Sect. 4 – in particular, see eq. (28). Perhaps the most noticeable result is that the decay into the lightest MSSM Higgs boson ($t \to c\,h^0$) is the one that can be maximally enhanced and reaching values of order $B(t \to c\,h^0) \sim 10^{-4}$ that stay fairly stable all over the parameter space. The reason for this dominance is that the decay $t \to c\,h^0$ is the one which is more sensitive to A_t, a parameter whose natural range reaches up to about $1\,TeV$. For more moderate values of A_t, however, the dominant Higgs decay mode can be $t \to c\,H^0$, but in this case the corresponding rate (also that of $t \to c\,A^0$) undergoes a rapid fall-off with M_{A^0} (Cf. Fig. 10b) as it was also the case in the unmaximized situation in Fig. 5d. In general, the (next-to-leading) dominance of $t \to c\,H^0$ in Figs. 10a and b is confined to a small corner of the parameter space which we pick up during the process of maximization. Quite in contrast, the FCNC top quark decay into the lightest Higgs scalar can have an observable ratio in a large portion of the parameter space, and in particular for almost all the range of Higgs boson masses. Needless to say, not all of the maxima can be simultaneously attained as they are obtained for different values of the parameters.

Moreover, we have also found (Cf. Fig. 10c) the maximum FCNC rate of the gluon channel in the MSSM. Under the RG-based assumption of only mixing in the LH sector, it reads

$$B^{\rm SUSY-QCD}(t \to c\,g) \lesssim \; 10^{-5}, \tag{33}$$

but it never really reaches the critical value 10^{-5}, which can be considered as the visible threshold for the next generation of colliders (see below). The visible limit for the gluon channel can only be picked up if one maximizes the ratio under the assumption of both LH and RH similar contributions, but even in this case the limit is only barely reached. However, we emphasize that the right order of magnitude can already be achieved with only flavor mixing in the LH sector. So for this decay we confirm the recent analysis of Ref.[28] in contrast to that of Ref. [15]. In Fig. 10c we have plotted the maximum value of $B(t \to c\,g)$ as a function of δ_{23} after scanning for the rest of the MSSM mass parameters within the $1\,TeV$ range. Interestingly enough we see that the maximum rate is not reached for the highest possible value of the flavor mixing parameter δ_{23}, the reason being that the physical squark masses – obtained after diagonalizing the 6×6 squark mass matrix in (flavor)$\times$(chiral) space – are constrained from below, so that the higher is δ_{23} the smaller is the maximally allowed value for the left-right mixing in the stop sector –a result which also holds for the case of the Higgs channels (1).

The remarkable enhancements obtained for the top quark FCNC Higgs decays (1) could bring them to detectable levels in large portions of the parameter space and not just in small optimized domains. To assess the discovery reach of the FCNC top quark decays in the next generation of accelerators we take as a guide the estimations that have been made for gauge boson final estates [33]. Using the information mentioned in Sect. 1 and assuming that all the FCNC decays $t \to c\,X$ ($X = V, h$) can be treated similarly, we roughly estimate the following sensitivities for $100\;fb^{-1}$ of integrated luminosity:

$$\textbf{LHC}: B(t \to c\,X) \quad \gtrsim \quad 5 \times 10^{-5}$$

$$\begin{aligned} \mathbf{LC}: B(t \to c\,X) &\gtrsim 5\times 10^{-4} \\ \mathbf{TEV33}: B(t \to c\,X) &\gtrsim 5\times 10^{-3}\ . \end{aligned} \tag{34}$$

Therefore, LHC seems to be the most suitable collider where to test this kind of phenomena. The LC is limited by statistics (due to much smaller top quark cross-section) but in compensation every collected event is clear-cut. So this machine could eventually be of much help, especially if we take into account that it could deliver 500 fb^{-1} per year [8] during the highest luminosity phase. In fact, a high luminosity e^+e^- super-collider offers the greatest potential for high precision top quark physics and it constitutes an ideal complement to concomitant LHC experiments. So, even if no SUSY particle is seen at LEP II, there is indeed a possibility to pin down quite a few FCNC $t \to c\,h$ and/or $t \to c\,g$ decays at the LHC first, and later on to perform a more detailed study at the LC. The situation with the Tevatron, as we see, is much more gloomy, since the required FCNC rates of $\sim 10^{-3}$ cannot be attained unless we artificially search in some remote (unnatural) corner of the parameter space. Hence, the Tevatron (even TeV33) seems to be of no much help in this regard, unfortunately.

Of course, with the range of SUSY masses that we have used in our analysis, one could try to detect some of the sparticles directly at the super-colliders. But this is always harder than dealing with conventional particles, and in any case the FCNC method is complementary to direct searches. Therefore, from the enormous experience gained in the study of top quarks, a dedicated analysis of the potential few hundred FCNC top quark decays per year at the super-collider LHC could provide a more clear identification of physical effects beyond the SM. This is so not only because the SUSY-FCNC rates could well be within the experimentally feasible ranges (34), as we have seen in our numerical analysis, but also because the signatures are likely to be separable from the background. For instance, at high $\tan\beta \gtrsim 30$ all of the final state Higgs bosons $h = h^0, H^0, A^0$ would mainly disintegrate into $b\bar{b}$ pairs, $h \to b\bar{b}$. These decays are also highly augmented as compared to the SM prediction, and include large MSSM radiative corrections [34]. Although there is an interval of Higgs masses where the alternative decay $h \to ZZ$ is possible and sizeable for an SM Higgs, this decay mode is not dominant for the SUSY Higgs bosons $h = H^0, A^0$ in the relevant region, and it is never kinematically accessible to h^0. In this region we expect that the FCNC final states $t\bar{t} \to c\,h, \bar{c}h$ are to be observed mainly as $c\,b\,\bar{b}$, $\bar{c}b\bar{b}$, and they should be effectively tagged through high p_T charm-quark jets and large invariant mass for the recoiling $b\bar{b}$ pairs. On the other hand, for moderately small $\tan\beta \gtrsim 1$ the situation is more cumbersome since the gluino-mediated FCNC rates for $t \to c\,h$ can be equally sizeable as for high $\tan\beta$, but in turn the decay pattern of the neutral Higgs bosons is much more complicated, and this is so the heavier are the Higgs bosons [35]. Notwithstanding, since in our case the Higgs bosons must satisfy $m_h < m_t$, it turns out that both the lightest CP-even and the CP-odd states $h = h^0, A^0$ still do preferentially decay into $b\bar{b}$ pairs. But not necessarily so the heavy CP-even Higgs H^0, for in this region it first cascades down predominantly (90%) into $h^0\ h^0$ (except in a narrow interval centered around $M_{H^0} = 130\,GeV$ where $H^0 \to b\bar{b}$ again dominates because the $H^0h^0h^0$-coupling changes sign); and as a result the observable $b\bar{b}$ pairs in the final state (emerging from the two secondary – real or virtual – decays $h^0 \to b\bar{b}$) are much softer than in the previous situation. Fortunately, we have seen that among the FCNC decays $t \to c\,h$ the one corresponding to $h = H^0$ is typically the most suppressed one, except in some corners of parameter space. In contrast, the most relevant decay (both under typical and optimized conditions) is that of $h = h^0$. The corresponding channel is always kinematically open in the MSSM and it can be tagged through the final state signature $c\,b\,\bar{b}$ mentioned above, which is dominant for any $\tan\beta > 1$. As for the FCNC decays in the gluon channel, $t \to c\,g$, here also a high p_T charm-quark jet against a highly energetic ($\sim m_t/2$) gluon jet is the indelible imprint of this decay. Altogether these features should be very helpful to mostly reduce all backgrounds and provide a clear-cut signal of rare top quark decays beyond the SM.

To conclude, the FCNC decays of the top quark are such rare events in the SM (especially the top quark decay into the Higgs boson) that their observation at detectable levels should be interpreted as an extremely robust indication of new physics. At present the most popular (phenomenologically compatible [23] and technically fully consistent [2]) quantum field theoretical extension of the SM is the MSSM; therefore, the effective tagging of FCNC top quark decays in the major accelerators round the corner could well be a first step into discovering SUSY. From our analysis we find that around the loci of maxima of the rates for the leading FCNC top quark decays, $t \to c\,h$ and $t \to c\,g$, we roughly have the following situation (under the assumption of flavor mixing only in the LH sector):

$$5 \times 10^{-6} \lesssim B(t \to c\,g)_{\max} < B(t \to c\,h)_{\max} \lesssim 5 \times 10^{-4}. \tag{35}$$

In both types of decays the dominant effects come from SUSY-QCD. However, it should not be undervalued the fact that the maximum electroweak rates for $t \to c\,h$ can reach the 10^{-6} level, which amounts not only to saying that they are 7 orders of magnitude greater than the maximum SM ones, but also to noticing that they are on the verge of being detectable. Last but not least, we stress once again that the largest FCNC rate both from SUSY-QCD and SUSY-EW is precisely that of the lightest CP-even state, a very fortunate fact which can hardly be overemphasized as $t \to c\,h^0$ is the only Higgs channel that is phase-space available across the whole MSSM parameter space.

At the end of the day, we should seriously bear in mind the possibility of observing FCNC decays of the top quark, and so we ought to be prepared to collect a few hundred, perhaps a few thousand, events of this sort at the LHC, together with a few dozen (although crystal-clear) $t \to c\,X$ ($X = h, g$) decays at the LC. If that would be the case, we could eventually find ourselves in the process of discovering SUSY dynamics at work before being able to directly produce (or clearly identify) any supersymmetric particle.

Acknowledgments: One of the authors (J.S.) is thankful to W. Bernreuther and D. Miller for updated information on the LC program. We are also grateful to M. Martínez for similar information. The work of J.G. has been supported in part by a grant of the Comissionat per a Universitats i Recerca, Generalitat de Catalunya No. FI95-2125. This work has also been financed by CICYT under project No. AEN95-0882.

References

[1] J.A. Coarasa, D. Garcia, J. Guasch, R.A. Jiménez, J. Solà, *Eur. Phys. J.* **C 2** (1998) 373.

[2] H. Nilles, *Phys. Rep.* **110** (1984) 1; H. Haber, G. Kane, *Phys.Rep.* **117** (1985) 75; A. Lahanas, D. Nanopoulos, *Phys. Rep.* **145** (1987) 1; See also the exhaustive reprint collection *Supersymmetry* (2 vols.), ed. S. Ferrara (North Holland/World Scientific 1987).

[3] J.A. Coarasa, J. Guasch, W. Hollik, J. Solà, *Phys. Lett.* **B 442** (1998) 326.

[4] J. Guasch, J. Solà, *Phys. Lett.* **B 416** (1998) 353.

[5] J. Solà, talk at the *Physics at Run II Supersymmetry/Higgs Workshop*, Fermilab, November 19-21, 1998; J.A. Coarasa, J. Guasch, J. Solà, UAB-FT preprint in preparation.

[6] D. Garcia, R. A. Jiménez, J. Solà and W. Hollik, *Nucl. Phys.* **B 427** (1994) 53; A. Dabelstein, W. Hollik, C. Jünger, R. A. Jiménez and J. Solà, *Nucl. Phys.* **B 454** (1995) 75.

[7] F. Gianotti, *Precision Measurements at the LHC*, proc. of the *IVth International Symposium on Radiative Corrections (RADCOR 98)*, Barcelona, 8-12 September 1998 (World Scientific 1999, to appear) ed. J. Solà.

[8] D.J. Miller, *Precision studies at a future linear collider*, [hep-ex/9901039] proc. of the *IVth International Symposium on Radiative Corrections (RADCOR 98),* Barcelona, 8-12 September 1998 (World Scientific 1999, to appear) ed. J. Solà; See also: *2nd Joint ECFA/DESY Study on Physics and Detectors for a Linear Electron-Positron Collider*, April 1998–March 1999, Orsay, Lund, Frascati and Oxford, `http://www.desy.de/conferences/ecfa-desy-lc98.html`, papers from the study to be published in DESY/ECFA report 123F.

[9] B. Mele, S. Petrarca and A. Soddu, *Phys. Lett.* **B 435** (1998) 401.

[10] G. Eilam, J.L. Hewett, A. Soni, *Erratum: Phys. Rev.* **D 59** (1998) 039901.

[11] G. Eilam, J.L. Hewett, A. Soni, *Phys. Rev.* **D 44** (1991) 1473.

[12] W.S. Hou, *Phys. Lett.* **B 296** (1992) 179; K. Agashe, M. Graesser, *Phys. Rev.* **D 54** (1996) 4445; M. Hosch, K. Whisnant, B.L. Young, *Phys. Rev.* **D 56** (1997) 5725.

[13] H. Fritzsch, *Phys. Lett.* **B 224** (1989) 423; B. Grzadkowski, J.F. Gunion and P. Krawczyk, *Phys. Lett.* **B 268** (1991) 106; N.G. Deshpande, B. Margolis and H. Trottier, *Phys. Rev.* **D 45** (1992) 178; M. Luke and M. Savage, *Phys. Lett.* **B 307** (1993) 387; D. Atwood, L. Reina and A. Soni, *Phys. Rev.* **D 55** (1997) 3156.

[14] C.S. Li, R.J. Oakes, J.M. Yang, *Phys. Rev.* **D 49** (1994) 293, *Erratum: ibid.* **D 56** (1997) 3156.

[15] G. Couture, C. Hamzaoui, H. König, *Phys. Rev.* **D 52** (1995) 1713; G. Couture, M. Frank, H. König, *Phys. Rev.* **D 56** (1997) 4213.

[16] J.L. Lopez, D.V. Nanopoulos, R. Rangarajan, *Phys. Rev.* **D 56** (1997) 3100.

[17] G.M. de Divitiis, R. Petronzio, L. Silverstini, *Nucl. Phys.* **B 504** (1997) 45.

[18] J.M. Yang, B. Young and X. Zhang, *Phys. Rev.* **D58** (1998) 055001; S. Bar-Shalom, G. Eilam and A. Soni, [hep-ph/9812518] (*Phys. Rev.* **D** to appear).

[19] J.F. Gunion, H.E. Haber, G.L. Kane, S. Dawson, *The Higgs Hunters' Guide* (Addison-Wesley, Menlo-Park, 1990).

[20] J. Ellis, G. Ridolfi, F. Zwirner, *Phys. Lett.* **B 262** (1991) 477; A. Brignole, J. Ellis, G. Ridolfi, F. Zwirner, *Phys. Lett.* **B 271** (1991) 123; H.E. Haber, R. Hempfling, *Phys. Rev. Lett.* **66** (1991) 1815; *Phys. Rev.* **D 48** (1993) 4280; M. Carena, J. Espinosa, M. Quirós, C. Wagner, *Phys. Lett.* **B 355** (1995) 209.

[21] P. Chankowski, S. Pokorski and J. Rosiek, *Nucl. Phys.* **B 423** (1994) 437; A. Dabelstein, *Z. Phys.* **C 67** (1995) 495; A. Dabelstein, *Nucl. Phys.* **B 456** (1995) 25.

[22] M. Carena, M. Quirós, C. Wagner, *Nucl. Phys.* **B 461** (1996) 407; H. Haber, R. Hempfling, A. Hoang, *Z. Phys.* **C 75** (1997) 539; S. Heinemeyer, W. Hollik, G. Weiglein, *Phys. Lett.* **B 440** (1998) 296.

[23] Talks by W. Hollik and G. Weiglein [hep-ph/9901317] in: *IVth International Symposium on Radiative Corrections (RADCOR 98),* Barcelona, 8-12 September 1998 (World Scientific 1999, to appear) ed. J. Solà.

[24] J.M. Yang, C.S. Li, *Phys. Rev.* **D 49** (1994) 3412, *Erratum: ibid.* **D 51** (1995) 3974.

[25] J. Guasch, in: *Quantum Effects in the MSSM* (World Scientific 1998, p. 256) (ISBN 981-02-3450-3) ed. J. Solà; J. Guasch, talk at the *2nd Joint ECFA/DESY Study on Physics and Detectors for a Linear Electron-Positron Collider*, 20th-23th March 1999, Oxford, U.K.; J. Solà, talk at the *Workshop on the LC Collider*, Sitges, Spain, April 28th-May 5th 1999.

[26] J. Guasch, J. Solà, *Z. Phys.* **C 74** (1997) 337.

[27] M.J. Duncan, *Nucl. Phys.* **B 221** (1983) 285; *Phys. Rev.* **D 31** (1985) 1139.

[28] F. Gabbiani, E. Gabrielli, A. Masiero, L. Silverstrini, *Nucl. Phys.* **B 477** (1996) 321.

[29] M. Misiak, S. Pokorski, J. Rosiek, *Supersymmetry and FCNC Effects*, in: "Heavy Flavours II", eds. A.J. Buras, M. Lindner, Advanced Series on directions in High Energy Physics, World Scientific 1998.

[30] A. Bouquet, J. Kaplan and C.A. Savoy, *Phys. Lett.* **B 148** (1984) 69; S. Bertolini, F. Borzumati, A. Masiero, G. Ridolfi, *Nucl. Phys.* **B 353** (1991) 591; C. Kolda, L. Roszkowski, J.D. Wells, G.L. Kane, *Phys. Rev.* **D 50** (1994) 3498.

[31] See the contributions by P. Giacomelli, M. Williams, A. Dominguez and R. Keranen, in: *Quantum Effects in the MSSM* (World Scientific 1998) (ISBN 981-02-3450-3) ed. J. Solà.

[32] J. Guasch, in: *Quantum Effects in the MSSM* (World Scientific 1998, p. 256) (ISBN 981-02-3450-3) ed. J. Solà.

[33] R. Frey *et al.*, *Top Quark Physics: Future Measurements*, preprint FERMILAB-CONF-97-085, April 1997 [hep-ph/9704243].

[34] J. A. Coarasa, R. A. Jiménez and J. Solà, *Phys. Lett.* **B 389** (1996) 312.

[35] A. Djouadi, in: *Quantum Effects in the MSSM* (World Scientific 1998, p. 197) (ISBN 981-02-3450-3) ed. J. Solà; M. Spira, *Fortsch. Phys.* 46 (1998) 203.

Figure Captions

Fig. 1 One-loop SUSY-EW vertex diagrams for the decay $t \to c\,h$ ($h = h^0, H^0, A^0$). Here d ($\tilde{d}_{\{a,b\}}$) represent mass-eigenstate down type quarks (squarks) of any generation.

Fig. 2 One-loop SUSY-EW diagrams contributing to the mixed $t-c$ self-energy, with a notation similar to that of Fig. 1.

Fig. 3 One-loop SUSY-QCD diagrams for the decay $t \to c\,h$: **(a)** vertex diagram, **(b)** mixed $t-c$ self-energy. $\tilde{u}_{\{\alpha,\beta\}}$ stand for mass-eigenstate up-type squarks of any generation.

Fig. 4 Evolution of the SUSY-EW contributions to the ratio (25) with **(a)** $\tan\beta$, **(b)** the trilinear coupling A_b, **(c)** the higgsino mass parameter μ, and **(d)** the pseudoscalar Higgs mass M_{A^0}. The rest of inputs are given in eq. (26).

Fig. 5 Evolution of the SUSY-QCD contributions to the ratio (25) with **(a)** the mixing parameter δ_{23} between the 2nd and 3rd squark generations, **(b)** the higgsino mass parameter μ, **(c)** the gluino mass $m_{\tilde{g}}$, and **(d)** the pseudoscalar Higgs mass M_{A^0}. The rest of inputs are given in eqs.(26) and (30).

Fig. 6 Evolution of the SUSY-QCD contributions to the ratio (25) with **(a)** the lightest sbottom mass ($m_{\tilde{b}_1}$), **(b)** the lightest stop mass ($m_{\tilde{t}_1}$), and **(c)** $\tan\beta$.

Fig. 7 Evolution of the SUSY-QCD effects on $B(t \to c\,g)$ as a function of **(a)** the mixing parameter δ_{23}, and **(b)** the gluino mass $m_{\tilde{g}}$. The results are shown under the assumptions of: mixing only in the left-handed squark sector (solid); and equal mixing in the left- and right-handed squark sectors (dashed).

Fig. 8 As in Fig. 7 but as a function of **(a)** the higgsino mass parameter μ, and **(b)** $\tan\beta$.

Fig. 9 As in Fig. 7 but as a function of **(a)** the lightest stop mass $m_{\tilde{t}_1}$ and **(b)** the soft SUSY-breaking trilinear top-squark coupling A_t.

Fig. 10 **(a)** Maximum value of $B(t \to c\,h)$, obtained by taking into account only the SUSY-EW contributions, as a function of M_{A^0} ; **(b)** as in (a) but taking into account only the SUSY-QCD contributions; and **(c)** maximum value of $B(t \to c\,g)$ as a function of the intergenerational mixing parameter δ_{23} in the LH sector. In all cases the scanning for the rest of parameters of the MSSM has been performed within the phenomenologically allowed region.

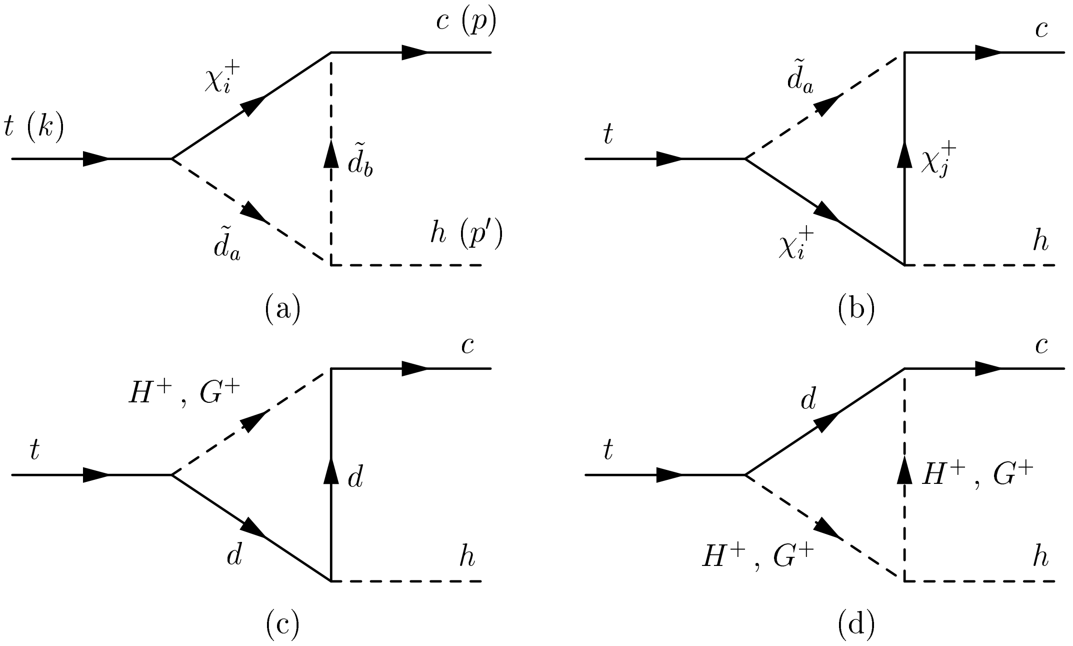
$t\ (k)$
χ_i^+
$c\ (p)$
$\tilde{d}_b$
$\tilde{d}_a$
$h\ (p')$
(a)
t
$\tilde{d}_a$
c
χ_j^+
χ_i^+
h
(b)
t
H^+ , G^+
c
d
d
h
(c)
t
d
c
H^+ , G^+
H^+ , G^+
h
(d)

Fig. 1

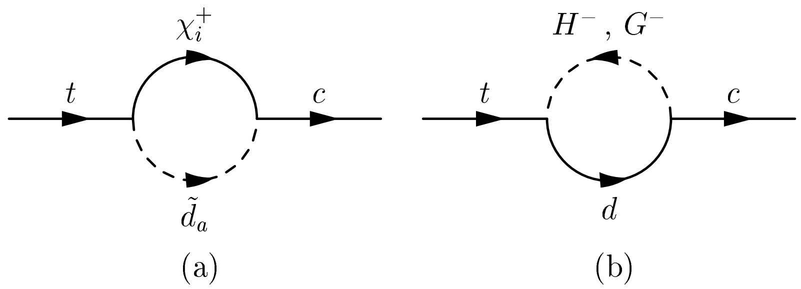
t
χ_i^+
c
$\tilde{d}_a$
(a)
t
H^- , G^-
c
d
(b)

Fig. 2

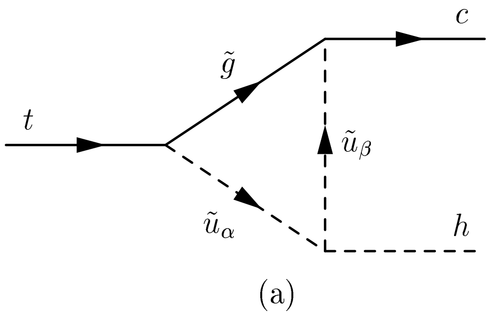

t
$\tilde{g}$
c
$\tilde{u}_\beta$
$\tilde{u}_\alpha$
h
(a)
t
$\tilde{g}$
c
$\tilde{u}_\alpha$
(b)

Fig. 3

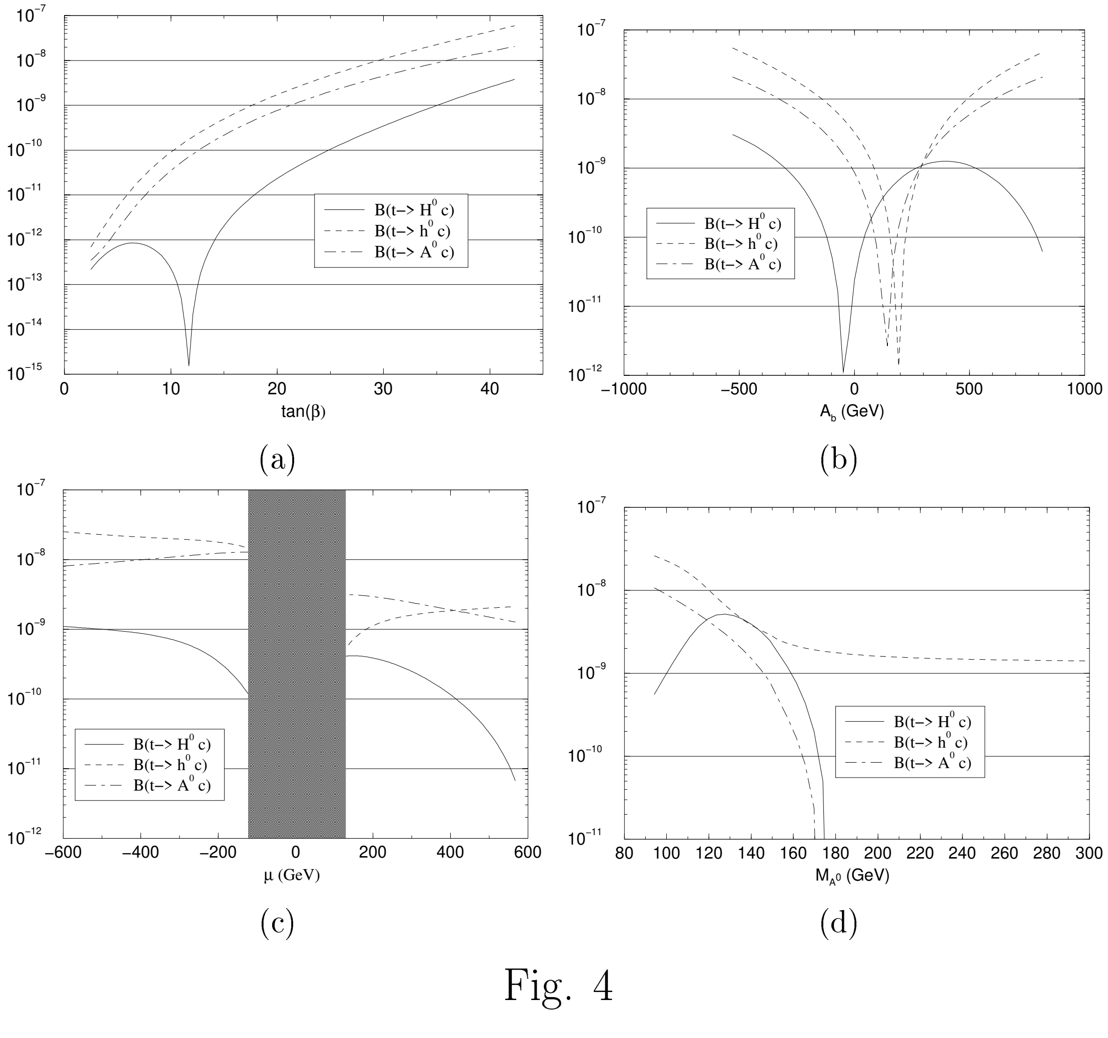

B(t−> H^0 c)
B(t−> h^0 c)
B(t−> A^0 c)
tan(β)
(a)
A$_b$ (GeV)
(b)
μ (GeV)
(c)
M$_{A^0}$ (GeV)
(d)

Fig. 4

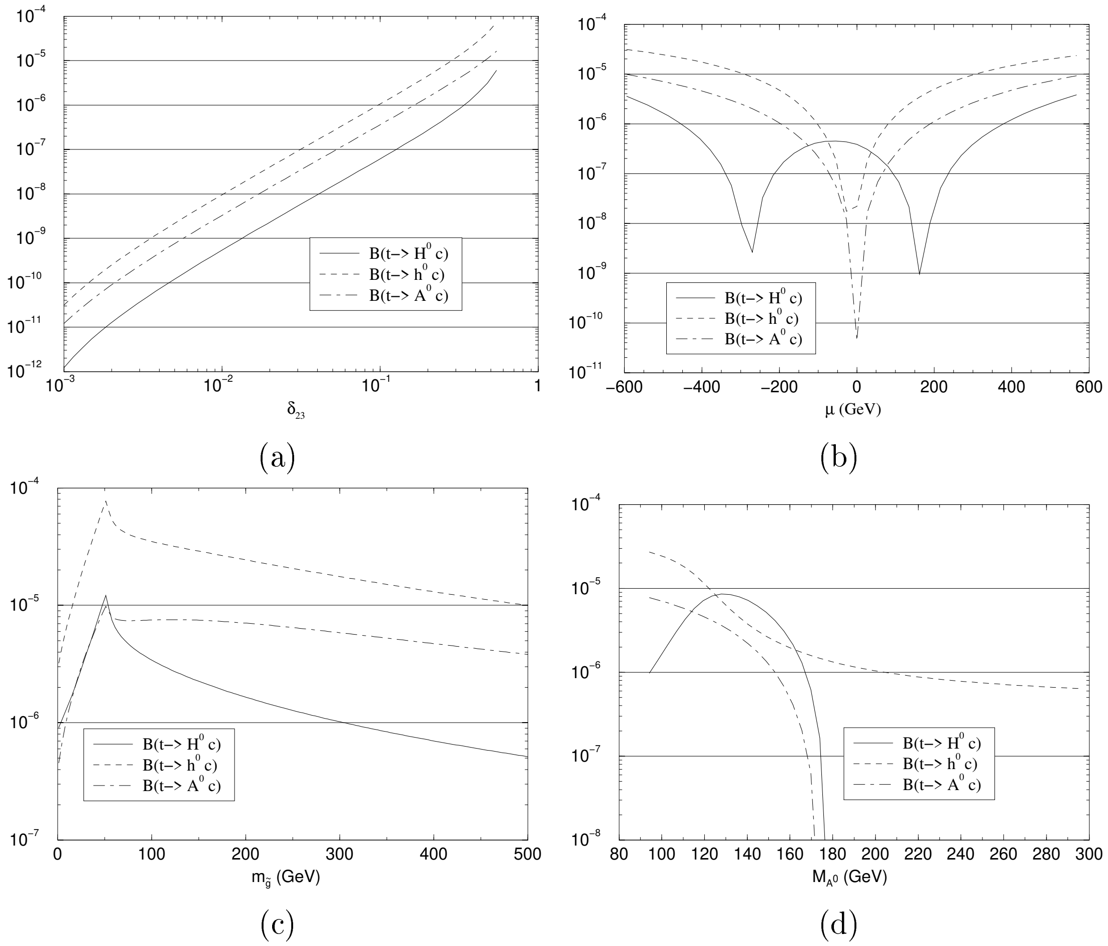

Fig. 5

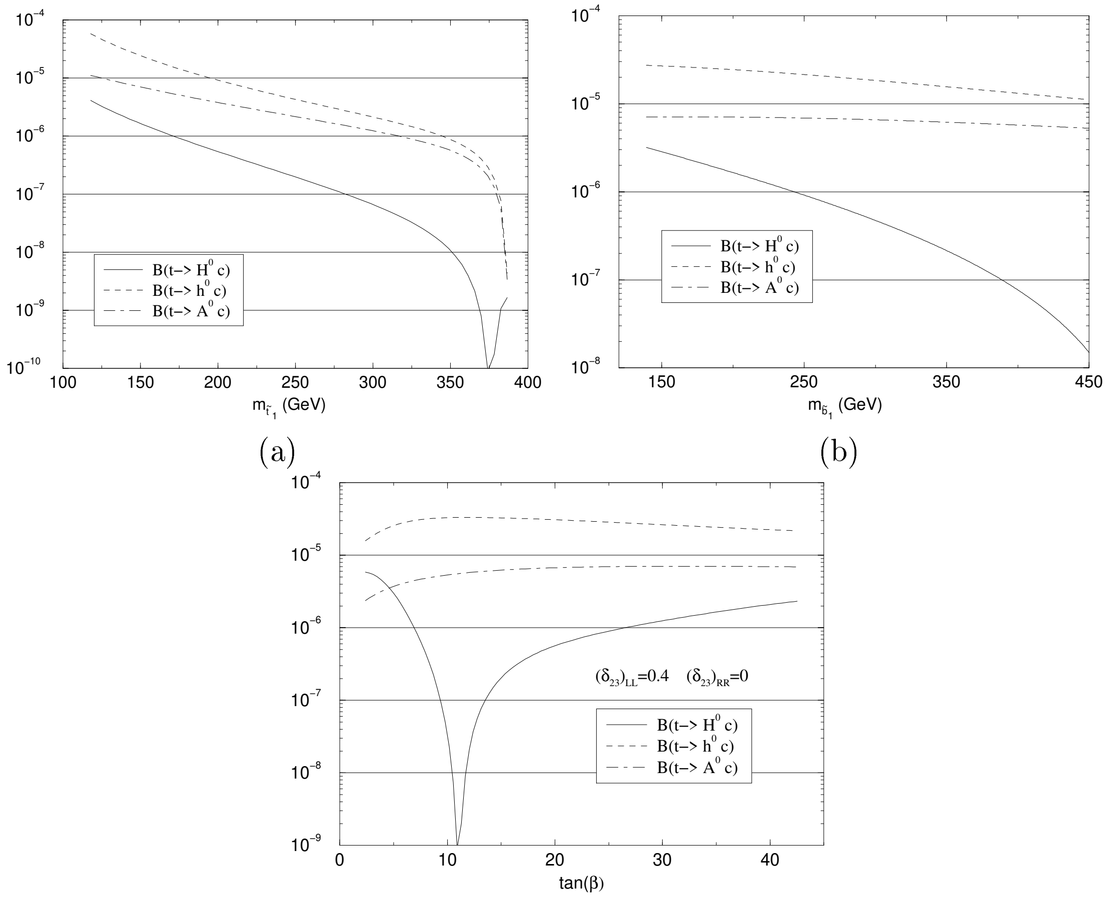

(a) (b)

(c)

Fig. 6

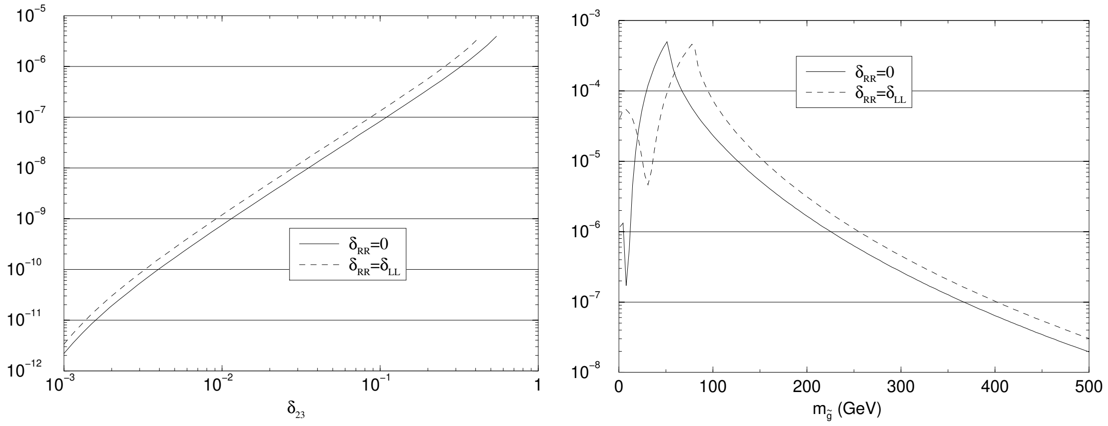

(a) (b)

Fig. 7

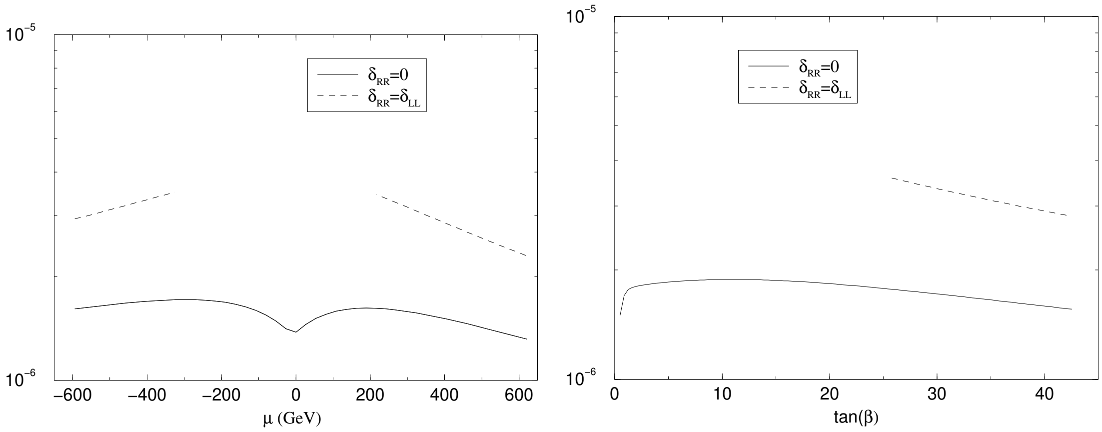

(a) (b)

Fig. 8

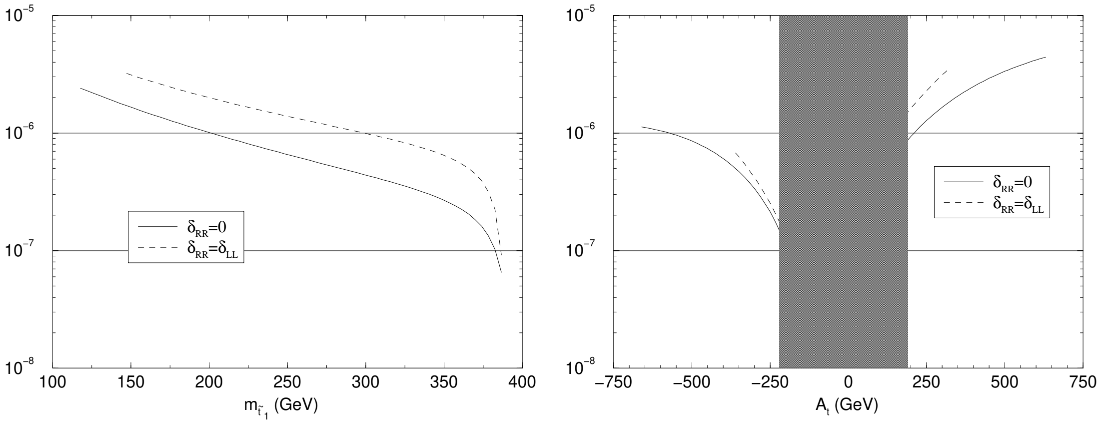

(a) (b)

Fig. 9

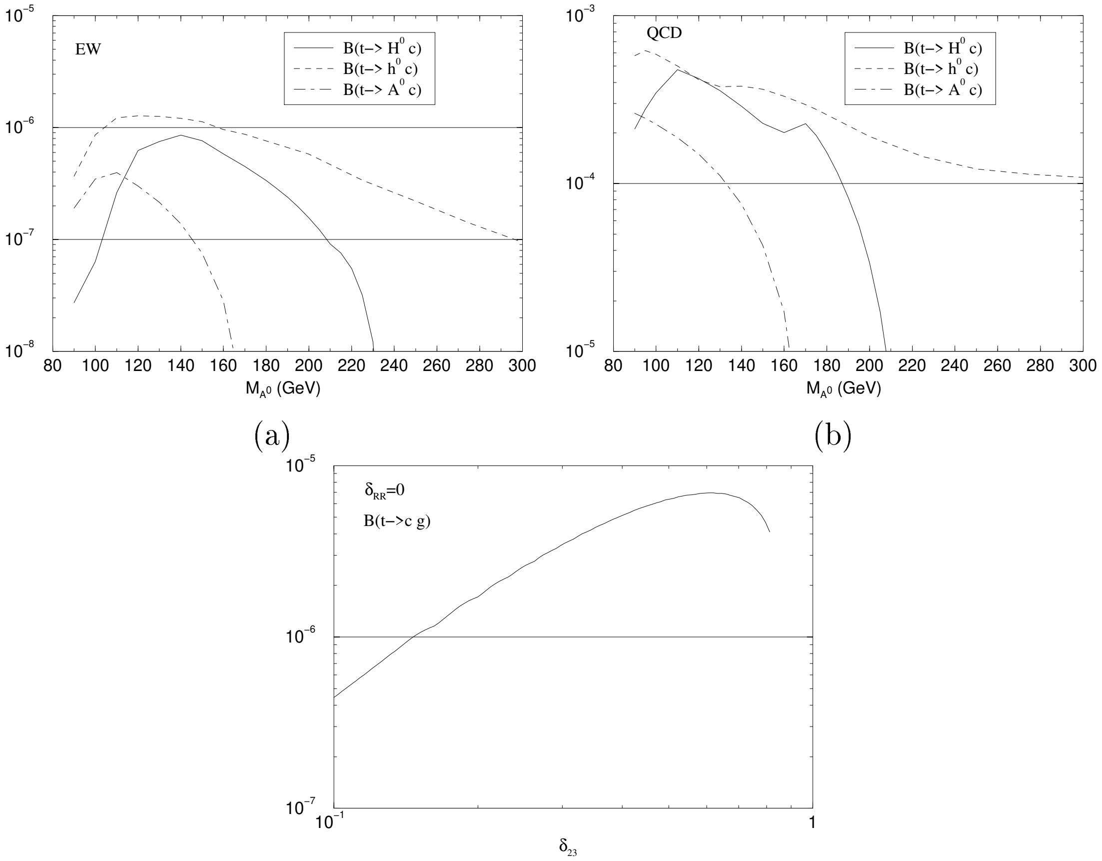
EW
B(t-> H^0 c)
B(t-> h^0 c)
B(t-> A^0 c)
M_A0 (GeV)
QCD
B(t-> H^0 c)
B(t-> h^0 c)
B(t-> A^0 c)
M_A0 (GeV)
δ_RR=0
B(t->c g)
δ_23

(a) (b)

(c)

Fig. 10